Aiolos Is Required for the Generation of High Affinity Bone Marrow Plasma Cells Responsible for Long-Term Immunity

Marta Cortés and Katia Georgopoulos

Cutaneous Biology Research Center, Massachusetts General Hospital, Harvard Medical School, Charlestown, MA 02129

Abstract

Antigenic encounter generates long-term immunity sustained by long-lived high affinity plasma cells resident in the bone marrow (BM). Here we show that the Ikaros family member, Aiolos, is specifically required for the generation of these plasma cells. Failure to generate high affinity plasma cells in the BM and to sustain serum antibody titers is apparent after both primary and secondary immunization of $Aiolos^{-/-}$ mice with a range of hapten concentrations. Chimera reconstitutions demonstrate that the BM plasma cell defect is B cell intrinsic. Lack of Aiolos does not alter expression of any of the previously described factors required for general plasma cell differentiation. No defect in somatic hypermutation, the generation of memory B cells, or short-lived high affinity plasma cells in the spleen was observed upon rechallenge. These studies support a model by which the high affinity plasma cell population in the BM undergoes a unique differentiation program that is dependent on Aiolos.

Key words: plasma cell subsets • long-term antibody production • immunologic memory • Aiolos • transcription factor

Introduction

One of the critical outcomes of primary exposure to Ag is the development of B cell memory. B cell memory is comprised of long-lived Ab-forming plasma cells (AFCs) and memory response precursors, both of which have undergone affinity maturation to provide Ag-specific immune protection. Long-lived Ab-secreting B cells accumulate in the BM shortly after primary immunization and are responsible thereafter for sustaining long-term systemic Ab production (1–3). Upon rechallenge with Ag, memory response precursors rapidly differentiate into AFC and produce high titers of high affinity Abs. The cellular origins and developmental pathways that give rise to these distinct populations of long-lived memory B cells have not been delineated.

Upon antigenic stimulation, mature naive B cells accumulate and proliferate in the margins of the splenic T cell zone, known as the periarteriolar lymphoid sheaths, where they enter one of two developmental pathways. In the first of these, naive B cells remain at the margins of the periarteriolar lymphoid sheaths and differentiate into short-lived AFCs (see Fig. 7). These cells are formed early in the response, peak at 8–10 d after immunization, and decline rapidly thereafter (4, 5). They produce low affinity Abs encoded by unmutated rearranged Ig genes. These low affinity extrafollicular AFCs have an immediate effector function that results in the quick clearance of Ag. In the second pathway, Ag-stimulated B cells migrate to the B cell follicle where they form a secondary follicle known as the germinal center (GC; for review see references 6 and 7). The GC is the site for affinity maturation of Ag-specific B cell clones and is characterized by histologically distinct light and dark zones. Within the dark zone of the GC, Ag-specific centroblasts undergo proliferation and somatic hypermutation that randomly diversifies their Ag receptor specificity. The fate of B cell clones that arise within the dark zone of the GC is determined by positive or negative selection in the light zone. A centrocyte will be rescued if it receives two survival signals: the first from follicular dendritic cells containing immune complexes on their complement receptor (CR2), and the second from Ag-specific T cells. It has been proposed that the fate of a centrocyte is determined by the intensity of signals it receives as it reencounters Ag on resident follicular dendritic cells: higher levels of B cell receptor (BCR) signaling select for high affinity variants, intermediate levels send B cells for recycling through the GC the potential benefit of additional mutations, whereas low levels signal

Address correspondence to Katia Georgopoulos, Cutaneous Biology Research Center, Massachusetts General Hospital, Harvard Medical School, Building 149, 13th Street, 3rd Floor, Charlestown, MA 02129. Phone: (617) 726-4445; Fax: (617) 726-4453; email: katia.georgopoulos@cbrc2.mgh.harvard.edu

death by apoptosis (6). It is from GC B cell clones selected for their high Ag affinity that high affinity AFCs and memory B cells arise.

2 wk after antigenic encounter, long-lived high affinity AFCs appear in the BM (3). Over time, these BM AFCs progressively increase in number and affinity, possibly due to post-GC affinity-driven clonal competition and selection events (6). The BM contains >90% of the high affinity AFCs (8) and is the primary source of high affinity serum Abs (3). As serum Abs have half-lives of <3 wk (9), the BM AFC population is responsible for long-term Ab production, and Ag-specific BM AFCs have been detected at least 1 yr after immunization (3, 8). Thus, the pathway leading to differentiation of high affinity AFCs in the BM is critical for long-term protective immunity.

Memory B cells arise later in the immune response, increasing in number as the GC declines, constituting a stable and distinct population at 21 d after immunization (10). Because the kinetics of long-lived AFC and memory B cell formation differs significantly, it is thought that they derive from distinct stages of the GC pathway (6). Long-lived BM AFCs do not proliferate upon secondary challenge, so their reported increase (8–10-fold) presumably arises from Ag-induced proliferation and differentiation of memory B cells (8). Recent efforts to delineate the origins and cellular composition of the memory B and long-lived AFC compartment have revealed considerable complexity and heterogeneity in both populations (6). The molecular mechanisms that regulate their induction and maintenance remain ill defined.

Aiolos is a member of the *Ikaros* gene family of nuclear regulators, presumed to function by modulating chromatin structure. In contrast to Ikaros, Aiolos expression is restricted to the B and T cell lineages and is not detected in nonlymphoid hematopoietic cell types. Unlike Ikaros, Aiolos deficiency does not affect early B cell differentiation in the BM, consistent with its absence or low expression relative to Ikaros at these early developmental stages (11, 12). In mature and recirculating B cells, however, Aiolos is expressed at much higher levels than Ikaros. Importantly, lack of Aiolos lowers the activation threshold of mature peripheral B cells in response to BCR and CD40 receptor engagement, thereby augmenting their proliferative capacity. These changes in B cell signaling and proliferation correlate with the increased number of GCs observed in aging Aiolos-deficient (Aio$^{-/-}$) mice in the absence of immunization (12). A deficit in marginal zone B cells is also detected in the Aio$^{-/-}$ mice and has been attributed to an altered signaling threshold in the newly emerged naive peripheral B cells (13). In addition, aging Aiolos mice develop nuclear autoantibodies and symptoms of systemic lupus erythromatosous, and exhibit an increased incidence of B cell lymphomas (12, 14).

In this investigation we examine the role of Aiolos in the development of Ag-specific T cell–dependent immunity using the hapten nitrophenyl (NP) response model. We show that Aiolos plays a critical role in the generation of BM AFCs required for long-lasting immunity. The BM AFC defects in Aio$^{-/-}$ mice are intrinsic to the B cell com-

partment and do not appear to involve previously described factors that regulate differentiation of all plasma cell subsets.

Materials and Methods

Mice and Chimeras.   Aio$^{-/-}$ mice (12) were backcrossed to C57BL/6 mice for nine generations. C57BL/6-Igh^a Thy1^a and RAG1$^{-/-}$ mice were purchased from Jackson ImmunoResearch Laboratories. For chimeras, 5×10^6 whole BM cells were injected into the tail vein of sublethally irradiated (950 rads) RAG1$^{-/-}$ mice. Recipient mice were injected with whole BM from WT C57BL/6-Igh^a Thy1^a mice, Aio$^{-/-}$ Igh^b Thy1^b mice, or a 50:50 mixture and maintained on antibiotic water. Mice were maintained under pathogen-free conditions and allowed to reconstitute for 6 wk before immunization.

Ags and Immunizations.   NP$_{22}$–chicken γ globulin (CGG; Biosearch Technologies) was precipitated in alum (AL(OH)3) at 4°C overnight at a concentration of 1 mg/ml NP-CGG. Mice were immunized i.p. with 50 μg NP$_{22}$-CGG conjugate precipitated in alum. An i.p. boost was performed with 50 μg NP$_{22}$-CGG 45 d after primary immunization. For chimeric mice, primary immunization was at 6 wk after reconstitution and the boost was 3 wk later.

ELISPOT.   The frequency of NP-specific AFCs in both the BM and the spleen was estimated by ELISPOT using two different coupling ratios of NP-BSA (Biosearch Technologies) as previously described (1).

Measurement of Serum Ab.   Abs specific for the NP hapten were detected by ELISA using NP$_4$-BSA and NP$_{23}$-BSA as previously described (1). Values are displayed as arbitrary units after subtracting the background from blocking buffer.

VH Gene Sequencing.   Single cell suspensions were prepared from the spleens of mice 13 d after primary immunization with NP. Cells were stained with anti–B220-PE and anti–GL-7–FITC and double positives were sorted into DNA lysis buffer. A two-step PCR strategy was used to exclude the recognition of V186.2-related gene segments and enrich specifically for V186.2. PCR products were cloned and sequenced with the V186.2-specific oligonucleotide used for PCR. For analysis of endogenous hypermutation at the J-C intron, cell suspensions were made from Peyer's patches of unimmunized WT and Aio$^{-/-}$ mice. DNA purified from GC B cells (B220$^+$ PNA^{hi}) was amplified and sequenced as previously described (15).

B Cell Purification.   Single cell suspensions were prepared from the spleens of unimmunized (4–5 wk) WT and Aio$^{-/-}$ mice. B cells were purified (90–95%) using an immunocolumn (Cedarlane).

Flow Cytometry.   Single cell suspensions were prepared from the femurs and spleen and Fc receptors were blocked with anti-CD16/CD32 Ab. Cells were stained with NP conjugated to allophycocyanin, anti-Igλ-PE, anti–B220-allophycocyanin, anti–CD138-PE, and FITC-conjugated anti-CD3ε, Mac-1, Gr-1, and Ter119. Chimeric mice were analyzed for reconstitution and relative B/T contribution by staining with anti–Thy1.1-FITC and anti–Thy1.2-PE or anti–Igh^a-FITC and anti–Igh^b-PE.

RT-PCR.   Purified B cells (10^6/ml) were cultured in RPMI with 20 μg/ml LPS (Sigma-Aldrich). After 4 d, total RNA was extracted and reverse transcribed using random primers. cDNA was amplified as follows: 25 cycles for 30 s at 94°C, 30 s at 60°C, and 60 s at 72°C. Primers used to PCR amplify Bcl-2, Bcl-x$_L$, Bcl-6, and β-actin have been described (16). Other primers designed to span an intron were: XBP-1 S: 5′-CGCAAGCG-GCAGCGGCTCACGCAC-3′ and XBP-1 A: 5′-GACTCAG-CAGACCCGGCCACCAGC-3′; Blimp-1 S: 5′-GTTCCCAA-

GAATGCCAACAGGAAG-3′ and Blimp-1 A: 5′-CACTGTG-AGCTCTCCAGGATAAGG-3′; IRF4 S: 5′-GTTCCGAGAA-GGGATCGACAAGCC-3′ and IRF4 A: 5′-GTGTGACTGG-TCAGGGGCATAATC-3′; c-Myc S: 5′-CGGGCAGACACT-TCTCACTGGACC-3′ and c-Myc A: 5′-CTTCCAGATA-TCCTCACTGGGCGC-3′; J-chain S: 5′-GGATCATCCCT-TCCACCGAGGATC-3′ and J-chain A: 5′-CTCACCAT-GATACCCAGGTGGGAC-3′; CXCR4 S: 5′-GTGATCCTG-GTCATGGGTTACCAG-3′ and CXCR4 A: 5′-GCTGAC-GTCGGCAAAGATGAAGTC-3′; and Fas S: 5′-GCACAG-AAGGGAAGGAGTACATGG-3′ and Fas A: 5′-CAAGGATG-GTCAACAACCATAGGC-3′. PCR reactions were performed in the presence of α-^{32}P-dCTP, and products were quantified using a PhosphorImager normalized to β-actin.

Results

Aio$^{-/-}$ Mice Mount a Normal Low Affinity AFC Response to Ag. To determine the role of Aiolos during an immune response, Aio$^{-/-}$ mice were immunized with the T cell–
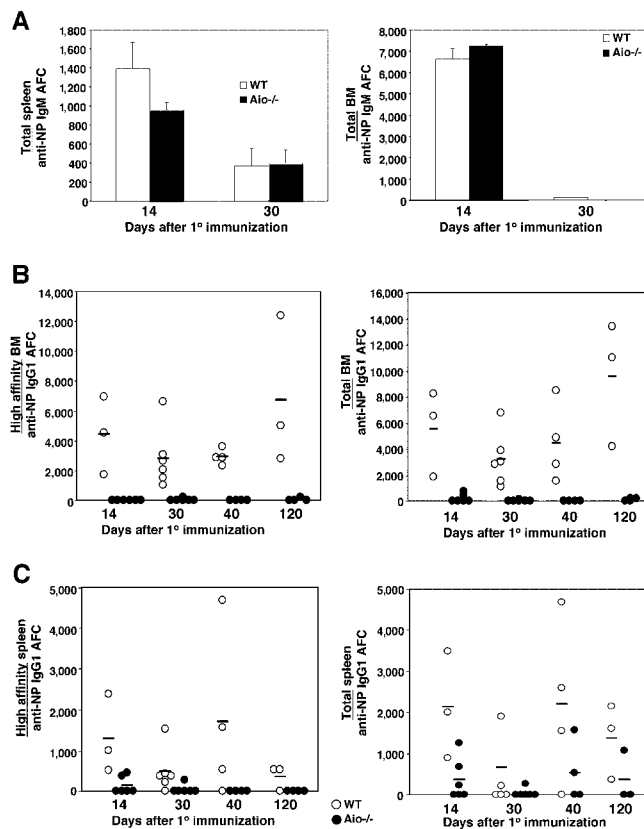

Figure 1. Impaired production of high affinity AFCs in Aio$^{-/-}$ mice after primary immunization. (A) Frequencies of NP-specific IgM-producing AFCs in the spleen (left) and BM (right) of WT (open bars) and Aio$^{-/-}$ (solid bars) at 14 and 30 d after primary immunization. IgG1-producing AFCs in the BM (B) and spleen (C) of WT (O) and Aio$^{-/-}$ (●) mice were measured at 14, 30, 40, and 120 d after primary immunization. Data were obtained from ELISPOT assays using NP$_4$ and NP$_{23}$ as the coating Ags. High affinity AFCs by NP$_4$ binding and total anti-NP AFCs were measured by NP$_{23}$ binding. Each point represents an individual mouse and results represent one experiment of at least three with similar findings. Horizontal bars in B and C indicate the average number of AFCs at each time point.

dependent Ag NP-CGG in alum. The Aio$^{-/-}$ mice used in this study were 3–5 wk of age, a time point before the "spontaneous" development of GC reactions, which form over time in the absence of immunization (12). The ligands NP$_4$-BSA or NP$_{23}$-BSA were used to determine the affinity of Abs produced by AFC in an ELISPOT assay. Densely haptenated NP (NP$_{23}$-BSA)–coated plates are bound by both high and low affinity anti-NP Abs, whereas sparsely haptenated BSA (NP$_4$-BSA)–coated plates are bound only by high affinity anti-NP Abs. Low affinity IgM-producing AFCs in the spleen and BM of Aio$^{-/-}$ mice were within physiological range at 14 d after immunization and declined by day 30 to levels similar to WT (Fig. 1 A). Thus, Aio$^{-/-}$ mice showed no defect in the production of low affinity AFCs during the primary response.

The Primary High Affinity AFC Response to Ag Is Impaired in Aio$^{-/-}$ Mice. 2 wk after primary immunization with NP-CGG, a significant number of high affinity IgG1-secreting AFCs (Fig. 1 B, left, 4,323 AFCs/total BM) was detected in the BM of WT mice, consistent with previous reports. At this time, high affinity AFCs constituted three fourths of the total AFCs in this location (Fig. 1 B, right). In sharp contrast, a very small number of IgG1-producing AFCs was detected in the BM of the Aio$^{-/-}$ mice, all of which were low affinity (Fig. 1 B, 197 NP$_{23}$ binding and no NP$_4$ binding). An almost 30-fold difference in the number of total BM AFCs was calculated between WT and Aio$^{-/-}$ mice (Fig. 1 B, 5,562 vs. 197 AFCs/total BM). To rule out the possibility that these differences are simply due to a delay in BM AFC production in Aio$^{-/-}$ mice, the number of high affinity AFCs was monitored over a period of 120 d after primary immunization (Fig. 1 B). Aio$^{-/-}$ mice showed no significant increase in high or low affinity AFCs over this period.

After primary immunization, high affinity IgG1-secreting AFCs were also present in the spleens of WT mice, although at a much lower frequency than in the BM. The number of IgG1 anti-NP–producing AFCs in the spleens of Aio$^{-/-}$ mice was lower than WT from 14 to 120 d after the primary response (Fig. 1 C). In addition, most AFCs detected in the Aio$^{-/-}$ spleens were low affinity, whereas, a significant number of high affinity clones were observed in the spleens of WT controls (Fig. 1 C).

Selection but Not Somatic Hypermutation Is Partially Impaired in the Aio$^{-/-}$ GC. To address whether the defect responsible for the high affinity AFC deficit in Aio$^{-/-}$ mice originates in the GC, the composition of GC B cells in Aio$^{-/-}$ versus WT mice was examined 13 d after primary immunization with NP. Early in the NP response, B cell clones present in the GC express Ig receptors with VH gene segments that belong to the V186.2 or V3 subgroups of the J558 VH family (17). Later in the NP response, the predominating B cell clones express a higher affinity Ig receptor containing the V186.2 gene segment that is referred to as canonical. GC B cells (B220$^+$/GL7$^+$) were isolated and 10,000–50,000 cell equivalents were amplified in a seminested PCR using V186.2-specific and JH2 intron prim-

Table I. *Sequence Analysis of Splenic GC B Cells from WT and Aiolos-null Mice Immunized with NP-CGG*

	No. sequences analyzed	Use of canonical V186.2 segment (%)	Sequences mutated (%)[a]	Average mutations per V gene (range)[a]	Position 33 Trp→Leu (%)[a]	R/S ratio CDR1/2[a]	YYSG/N CDR3 (%)[a]
WT	37	34 (92)	97	3.1 (0–11)	41	10.6	44
Aio$^{-/-}$	60	25 (41)	68	1.4 (0–3)	8	5.3	24

Sorted GC B cells (B220$^+$ GL-7$^+$) were cloned and the sequences from 60 Aio$^{-/-}$ and 37 WT clones were analyzed.
[a]Values from rearrangements using the canonical Vh186.2 sequence only.

ers, and then cloned products were sequenced. Both canonical and noncanonical members of the V186.2 and V3 gene subfamilies can be detected by this amplification strategy due to sequence conservation in their respective promoters. Consistent with previous reports (17), 92% of independent B cell clones obtained from WT GCs contained productive V(D)J rearrangements using the V186.2 gene segment (Table I, 34 out of 37). In contrast, only 41% (Table I, 25 out of 60) from Aio$^{-/-}$ mice used the canonical V186.2 sequence. Analysis of the remaining clones from Aio$^{-/-}$ GC B cells revealed gene segments encountered early in the NP response that are normally selected out by day 14 due to their lower Ag affinity. These noncanonical VH gene segments are other members of the V186.2 and V3 gene subfamilies, namely CH10, V223, C1H4, 4m114, and 165.1.

Analysis of the canonical V186.2 gene sequences from Aiolos and WT GC B cell clones revealed that 68% were mutated in the Aio$^{-/-}$ B cell population, whereas almost all (97%) were mutated in the control population (Table I). The tryptophan to leucine (W→L) replacement at position 33 in the CDR1 of V186.2 provides a dramatic increase in the NP affinity of V186.2 and is considered a hallmark of clonal selection (17, 18). Of the Aio$^{-/-}$ GC B cell clones with a canonical V186.2 gene segment, only 8% had the W→L mutation versus 41% percent of the V186.2-bearing WT clones (Table I). In addition, only 24% of the V186.2-containing sequences had the affinity-enhancing YYGS/N motif in the CDR3 of Aio$^{-/-}$ GC B cells versus 44% in WT.

During the course of a typical GC reaction, the ratio of amino acid replacement to silent mutations (R/S) in the CDRs and framework regions of the VH genes of NP-specific B cells changes in a manner consistent with selection for improved Ag binding. Namely, it increases in the former and decreases in the latter. The R/S ratio in the CDR1–2 of the Aio$^{-/-}$–derived V186.2 sequences was 5.3, whereas for the WT-derived sequences it was 10.6 (Table I), consistent with strong selection for higher affinity receptors (18).

Although normal selection among Aio$^{-/-}$ GC B cells is clearly impaired, it is possible that additional defects in somatic hypermutation are responsible for the lower frequency of mutations observed among the canonical sequences derived from Aio$^{-/-}$ GC B cells. To address this possibility, Peyer's patch GC B cells were isolated and ana-

lyzed for unselected mutations at the intronic 3′ flank of the VH segment. Because the mutations analyzed are within the J$_H$-C$_H$ intron (15), this approach allows for a study of the mutational process without the skewing effects of antigenic selection and potential complications arising from multiple V gene usage. A similar proportion of sequences analyzed from Aio$^{-/-}$ and WT B cells contained mutations (Table II, 96 vs. 97%). The frequency of mutations was also similar (Table II, 14.7 mutations/10^3 bp in Aio$^{-/-}$ vs. 11.2/10^3 bp in WT).

Taken together, these studies indicate that Aio$^{-/-}$ mice have no intrinsic defect in somatic hypermutation, but exhibit impaired B cell selection within the GC that reduces but does not ablate the emergence of high affinity B cell variants from the GC.

Antigenic Rechallenge Reveals Memory B Cells but Not BM AFCs in Aio$^{-/-}$ Mice. To determine whether memory B cell formation was affected in Aio$^{-/-}$ mice, the frequency of NP-binding Igλ$^+$ B lymphocytes was analyzed by flow cytometry 6 d after boost. Although NP-specific B cells were undetectable before immunization, they were present at similar numbers in WT and Aio$^{-/-}$ spleens (Fig. 2 A) and BM (not depicted) after secondary immunization. These cells do not express CD138 or other plasma cell markers (not depicted).

Consistent with the expansion of memory B cells after restimulation, the number of high affinity AFCs in the spleens of WT mice was also dramatically increased 6 d after boost (Fig. 2 B). A similar increase was observed in the spleens of Aio$^{-/-}$ mice at this time (Fig. 2 B, 13,896 in Aio$^{-/-}$ vs. 16,246 in WT). This population of splenic

Table II. *Mutation Frequency in Peyer's Patch GC B Cells*

	No. sequences analyzed	Sequences mutated (%)	Total no. of mutations	Mutation frequency of mutated clones (×10^{-3})
WT	25	96	59	11.2
Aio$^{-/-}$	31	97	97	14.7

Sorted GC (B220$^+$ PNA$^+$) B cells from Peyer's patches were cloned and the J to C intronic sequence for 31 Aio$^{-/-}$ and 25 WT clones was analyzed.
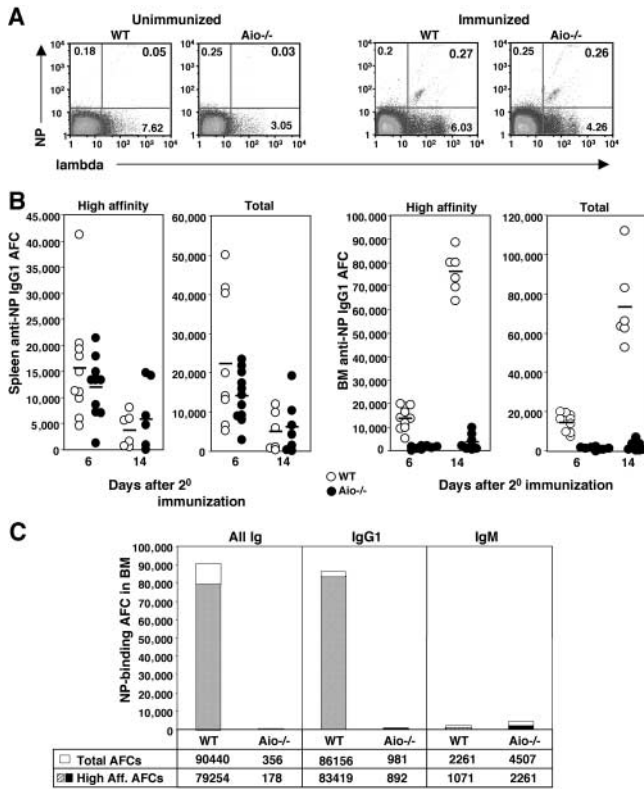
Figure 2. Antigenic reexposure supports transient expansion of high affinity AFCs in the spleen but not in the BM. FACS® analysis of spleen cells from WT and Aio$^{-/-}$ mice before and 6 d after secondary immunization (A). Cells were gated within the lineage-negative compartment and examined for NP binding and expression of Ig light chain. (B) Frequencies of NP-specific IgG1-producing AFCs in the spleen (left) and BM (right) of WT (○) and Aio$^{-/-}$ (●) mice were examined at 6 and 14 d after boost. Data were obtained from ELISPOT assays using NP$_4$ (high affinity) and NP$_{23}$ (total) as the coating Ags. Each point represents an individual mouse and data is from one experiment of at least three with similar results. (C) BM NP-specific AFCs of IgE, IgA and IgG isotypes, IgG1 isotype, and IgM isotype were quantified 14 d after 2° immunization. High and low affinity anti-NP AFC (NP$_{23}$ binding) are represented by open bars. High affinity (NP$_4$ binding) anti-NP AFCs comprise the hatched and solid portion of the bars.

AFCs, however, was relatively short-lived, as it had significantly declined by day 14 in both WT and Aio$^{-/-}$ mice.

In WT mice, the BM AFC expansion triggered by secondary antigenic encounter is more than 10-fold greater to that seen during primary response (compare Figs. 1 B and 2 B). In sharp contrast, restimulation with Ag failed to increase the high affinity AFCs in the BM of Aio$^{-/-}$ mice, which remained as low as after primary stimulation (Fig. 2 B). By day 14 after restimulation, there was a 30-fold difference in the frequency of the high affinity anti-NP AFCs of IgG1 isotype produced in the BM of Aio$^{-/-}$ compared with WT mice (Fig. 2 B, 2,806 vs. 73,398, respectively).

To rule out the possibility that in the absence of Aiolos high affinity Ag receptors switch to a different isotype than the one normally induced by NP on a WT C57BL/6 background, the frequency of high affinity AFCs was measured for all Ig isotypes. A minimal amount of high affinity AFCs

of IgE, IgA, and IgG isotypes was detected in Aio$^{-/-}$ mice 14 d after secondary immunization (Fig. 2 C, left). As expected, a large number of AFCs was present in the BM of WT littermates, all of which produced high affinity anti-NP IgG1 (Fig. 2 C, left and middle). The only anti-NP AFCs present in the Aio$^{-/-}$ BM was a small population secreting low affinity IgM (Fig. 2 C, right). These AFCs are likely the result of a primary response generated during the course of secondary immunization.

To evaluate the overall ability of Aio$^{-/-}$ mice to mount a high affinity AFC response, the total number of AFCs (mostly obtained from BM and spleen) was examined. After the first encounter with Ag, the total number of high
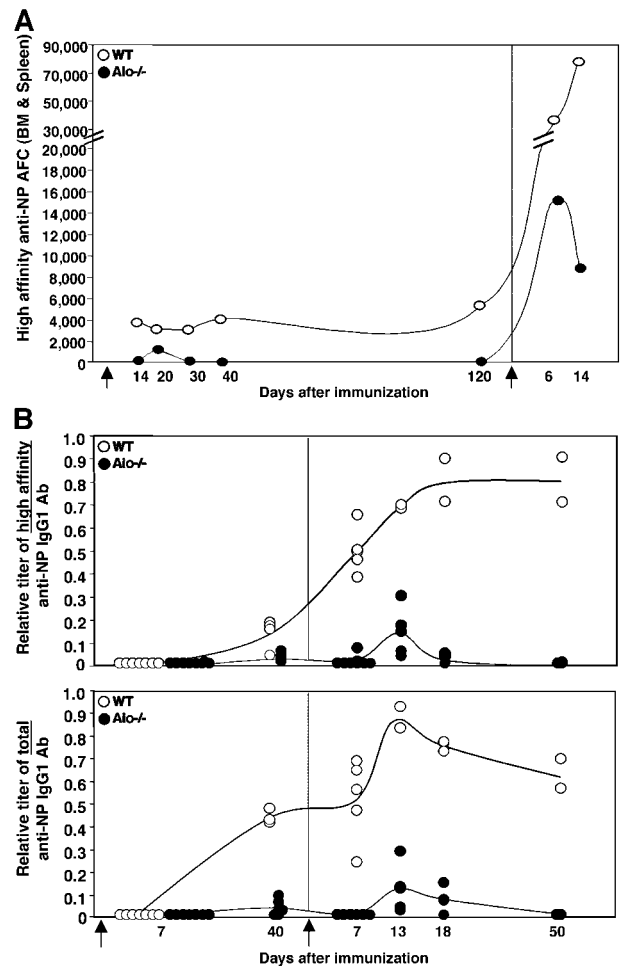

Figure 3. Severe reduction in the total numbers of AFCs and Ab titers during primary and secondary immune responses in Aio$^{-/-}$ mice. (A) Kinetics of high affinity NP-specific IgG1-producing AFCs in the BM and spleen of immunized WT (○) and Aio$^{-/-}$ (●) mice. (B) Kinetics of NP-specific IgG1 serum Ab of high (top) or all (bottom) affinity of WT (●) or Aio$^{-/-}$ (○) mice at the indicated times. The relative titers of anti-NP Ab were measured by ELISA using either NP$_4$ (top) or NP$_{23}$ (bottom) as the coating Ag. Each point represents an individual mouse (day 7, $n = 7$; day 40, $n = 4$ for WT; $n = 6$ for Aio$^{-/-}$; day 7 after 2°, $n = 5$ for WT and $n = 7$ for Aio$^{-/-}$; day 13 after 2°, $n = 3$ for WT and $n = 4$ for Aio$^{-/-}$; days 18 and 50 after 2°, $n = 3$) and data are from one of at least three representative studies. The arrows represent time of immunization.

affinity NP-specific AFCs in Aio^{−/−} mice was on average 10-fold lower than WT (Fig. 3 A, from day 14 to 120). After rechallenge with Ag, an increase was initially seen in the total number of high affinity AFCs in the Aio^{−/−} mice, which was accounted for by the splenic compartment. This increase was short-lived, however, and by day 14 the difference in total AFCs between WT and Aio^{−/−} mice increased to ninefold (Fig. 3 A). Thus, although memory B cells are produced in Aio^{−/−} mice and upon recall can differentiate into short-lived high affinity splenic AFCs, they fail to generate the long-lived high affinity AFC population in the BM.

The High Affinity Serologic Response to Ag Is Also Impaired by Aiolos Deficiency. AFCs in the spleen, BM, and possibly other sites together contribute to the titer of high affinity serum Abs. Before immunization, Aio^{−/−} and WT mice exhibited similar levels of total serum IgM and IgG and no detectable anti–NP Abs (not depicted). After immunization, and consistent with the profound defect in BM AFC activity, the titers of high affinity anti–NP IgG1 Abs in the serum of Aio^{−/−} mice were low compared with WT and remained low for an extended period of time (Fig. 3 B). 13 d after secondary immunization, a small transient increase in the levels of high affinity NP-specific IgG1 Ab was detected in the serum of Aio^{−/−} mice. This increase in Ab titers correlates with the appearance of the short-lived splenic AFC population in the Aio^{−/−} mice upon rechallenge (compare A and B in Fig. 3). However, Abs have a short half-life and continuous secretion by AFCs is required to maintain their serum level. Because the only high affinity AFCs present in the Aio^{−/−} spleen were short-lived, so was the serum Ab, and by day 50 after secondary immunization the titers of Ag-specific Ab were reduced to background levels.

Different Doses of Ag Fail to Reveal High Affinity BM AFCs in Aio^{−/−} Mice. B cells from Aio^{−/−} mice undergo augmented in vitro proliferative responses upon BCR and CD40 ligation (12). It is therefore possible that the impairment in the NP response in Aio^{−/−} mice was due to excessive BCR signaling triggered by the levels of immunizing Ag, which caused an aborted response. To examine this possibility, mice were immunized with lower doses of Ag (1 and 10 μg NP-CGG). The response was measured by both the AFC frequency in the BM and spleen of immunized animals and by the anti–NP Ab serum titers. At lower doses of immunizing Ag, there was a diminished anti–NP response in WT mice and almost no response in Aio^{−/−} mice (not depicted). Aio^{−/−} mice were also immunized with high doses of Ag (100 μg NP-CGG). The results followed a similar trend to those obtained at lower doses (10 and 50 μg) of immunizing Ag (not depicted). These studies demonstrate that Aiolos deficiency impairs BM AFC generation and that different levels of antigenic stimulation are not sufficient to overcome the defect.

The Defect in BM AFC Formation in Aio^{−/−} Mice Is Intrinsic to B Cells. Aiolos is not only expressed in B cells but also in T cells (11). Generation and maintenance of high affinity AFCs in the BM is dependent on adequate T cell help
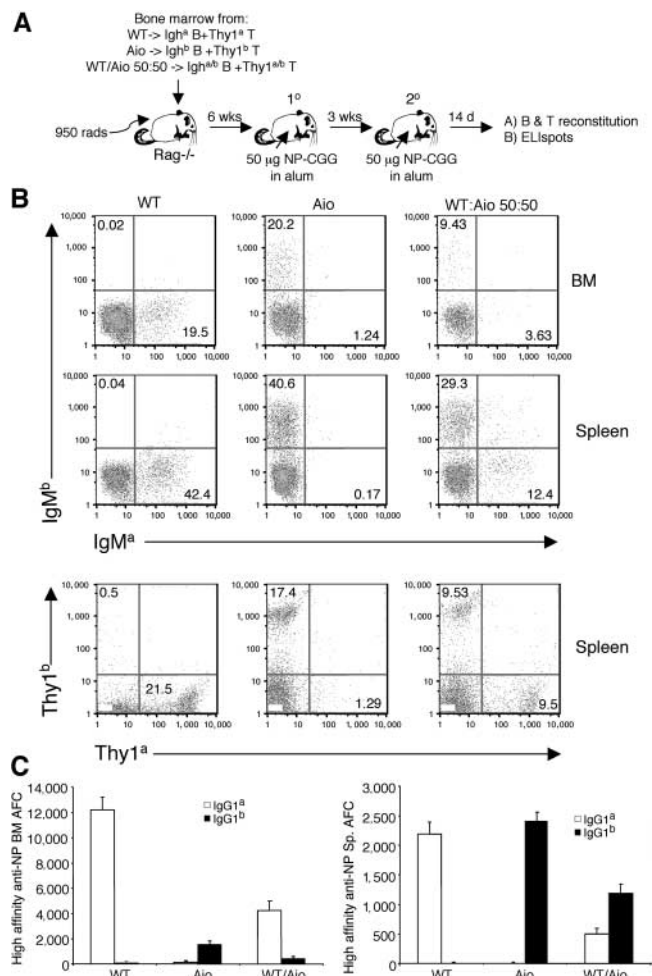

Figure 4. The deficiency in high affinity AFC production in Aio^{−/−} mice is B cell intrinsic. (A) BM from WT, Aio^{−/−}, or a 50:50 mixture of the two was used to reconstitute irradiated RAG^{−/−} chimeras. Mice were immunized from 6 to 9 wk after reconstitution and analyzed 14 d after boost. (B) Flow cytometric analysis of haplotype-specific expression of IgM and Thy1 molecules in the reconstituted chimeras. BM and spleens were stained with anti-IgM[a] (WT-derived) and anti-IgM[b] (Aio^{−/−} derived) to determine B cell contributions. Spleens were stained with anti-Thy1[a] (WT-derived) and anti-Thy1[b] (Aio^{−/−}-derived) Abs to determine T cell contributions. (C) IgG1-producing AFCs in the BM (left) and spleen (right) of WT (open bars) and Aio^{−/−} (solid bars) were measured 14 d after secondary immunization with 50 μg NP-CGG. Data were obtained from ELISPOT assays using NP4 as the coating Ag. The revealing Abs used were specific for WT-derived (anti-IgG1[a]) or Aio^{−/−}-derived (IgG1[b]) AFCs.

and BM stromal support (6). To determine whether the AFC deficit in Aio^{−/−} mice was intrinsic to B cells or due to a defect in T cell help or stromal support, BM chimeras were generated. Irradiated RAG1^{−/−} recipients were adoptively transferred with whole BM from WT C57BL/6-Igh[a] Thy1[a] mice, Aio^{−/−} Igh[b] Thy1[b] mice, or a 50:50 mixture of WT and Aio^{−/−} cells. 6 wk after reconstitution, mice were immunized with 50 μg NP-CGG in alum, boosted at 3 wk, and killed 14 d later (Fig. 4 A). Analysis of BM and spleen populations in the RAG1^{−/−} chimeras revealed a normal number of reconstituted B and T cells. All B cells

from WT-reconstituted mice were of the Igh[a] haplotype, whereas B cells from Aio^{−/−}-reconstituted mice were of the Igh[b] haplotype (Fig. 4 B, IgM[a] vs. IgM[b]). Mice that had received a 50:50 BM mixture from WT and Aio^{−/−} mice had B cells of both the Igh[a] and Igh[b] haplotype. This was also the case for T cells, which were Thy1[a] in WT, Thy1[b] haplotype in Aio^{−/−}, and an equal mixture of Thy1[a]/Thy1[b] in the 50:50 chimeras (Fig. 4 B). However, although T cells in the 50:50 chimeras were equally derived from WT and Aio^{−/−} cells, there was a bias toward the generation of Aio^{−/−}-derived B cells (∼3:1 ratio for Aio/WT instead of the expected 1:1; Fig. 4 B). This result did not, however, affect our ability to evaluate whether WT T cells, B cells, or BM could correct the Aio^{−/−} AFC phenotype.

Analysis of the reconstituted mice revealed a significant number of WT-derived BM AFCs in both WT and WT/Aio^{−/−} chimeras (Fig. 4 C, left, IgG1[a]). The lower number of WT AFCs seen in WT/Aio^{−/−} chimeras correlates with the overall lower number of Igh[a] B cells present in these mice. In spite of the normal or increased Aio^{−/−} B cell reconstitution in chimeras, their contribution to high affinity anti-NP AFCs in the BM was very limited (Fig. 4 C, left, IgG1[b]). In contrast, the number of splenic AFCs was similar in the three groups (Fig. 4 C, right, IgG1[a] and IgG1[b]), consistent with previous findings that Aio^{−/−} mice generate splenic AFCs at normal frequencies after secondary immunization (Fig. 2 B). Thus, the deficiency in high affinity AFCs in the BM of Aio^{−/−} mice is not due to insufficient T cell help, stromal support, or potential interactions with other B cell populations. Rather, it reflects an intrinsic requirement for Aiolos in the development of this specific subset of long-lived plasma cells.

Aiolos-deficient B Cells Do Not Exhibit Defects in Known Plasma Cell Differentiation Markers. Given that AFC populations are primarily operationally defined, we examined the ability of Aio^{−/−} B cells to differentiate into plasma cells in vitro. After 4 d of LPS stimulation of purified splenic B cells, we examined Ig levels in the culture supernatants. Although a decrease in IgM and IgG3 production was observed in Aio^{−/−} cultures, there was no overall difference in the ability to produce different Ig isotypes under these conditions (Fig. 5 A). Similar results were obtained in B cell cultures treated with anti-CD40 or anti-CD40 and IL-4, stimuli that recapitulate the in vivo physiological response (not depicted). We also examined the expression of gene products whose activity has been shown to be critical for the differentiation of all plasma cells. *XBP-1*, *Blimp-1*, and *IRF-4* are transcriptional regulators required in this process. The J chain is up-regulated upon plasma cell differentiation and is required for IgM and IgA secretion (19). Similar increases in the transcripts of three of the four genes were detected in cultures of Aio^{−/−} and WT B cells stimulated for 4 d with LPS (Fig. 5 B). A greater induction of *IRF-4* was detected in the Aio^{−/−} cultures.

The high affinity BM AFC population is thought to originate within the GC. Therefore, we probed the Aio^{−/−}

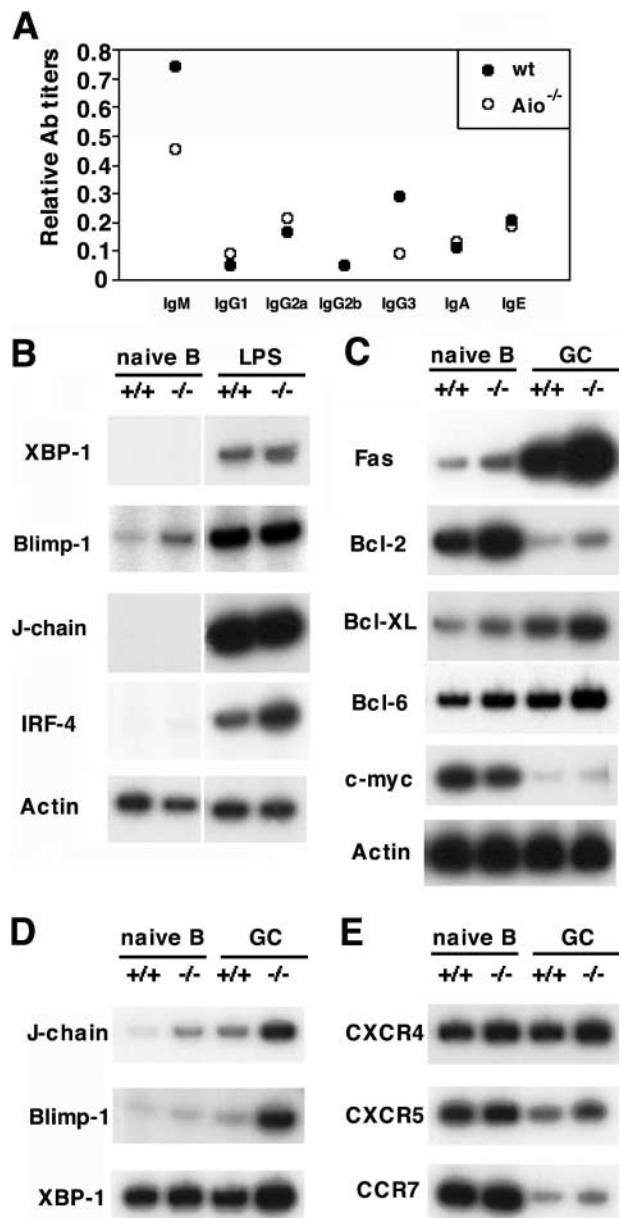**Figure 5.** The ability of Aio^{−/−} B cells to express plasma cell–specific and survival genes is unaffected. (A) Culture supernatants of purified B cells stimulated with LPS were assayed for production of different isotypes. Each point represents the average titer of a purified B cell culture from a pool of five mice. (B) RT-PCR analysis was performed on naive purified B cells as well as on LPS-stimulated cultures for *XBP-1*, *Blimp-1*, *J-chain*, and *IRF-4*. *Actin* was used as a control in all samples. (C–E) RT-PCR analysis was performed on sorted naive B cells (B220[+] PNA[−]) and GC B cells (B220[+] PNA[+]) from WT and Aio^{−/−} mice for *Fas*, *Bcl-2*, *Bcl-xL*, *Bcl-6*, *c-myc* (C), *J-chain*, *Blimp-1*, *XBP-1* (D), *CXCR4*, *CXCR5*, *CCR7* (E), and *actin*.

GC B cell compartment for changes in gene expression that may underlie the AFC deficit. We were particularly interested in factors that have been reported to be important in clonal selection or survival of the memory B and AFC populations. The level of the apoptotic factor *Fas* in the Aio^{−/−} GC B cells was significantly higher than in WT

counterparts (average 2.5-fold increase; Fig. 5 C). A three-fold increase in *Fas* was also observed in LPS-stimulated Aio$^{-/-}$ B cell cultures (not depicted). A small but consistent increase in the antiapoptotic factor *Bcl-2* was also observed. No significant changes in *Bcl-x$_L$*, *Bcl-6*, or *c-myc* were seen between WT and Aio$^{-/-}$ GC B cells (Fig. 5 C). Recent studies have shown that a small fraction of GC B cells express plasma cell–associated genes such as *Blimp-1* and *J chain*, indicating commitment to the plasma cell lineage (20). In WT mice, a small increase in the expression of *Blimp-1* and *J-chain* was observed from naive to GC B cells. Interestingly, this increase was seen at a more pronounced level in Aio$^{-/-}$ GC B cells (Fig. 5 D), indicating that plasma cell differentiation is taking place.

It is possible that centrocytes exit the GC and differentiate into plasma cells but cannot migrate to the BM. To test the possibility of a possible homing defect, GC populations were also examined for expression of chemokine receptors.
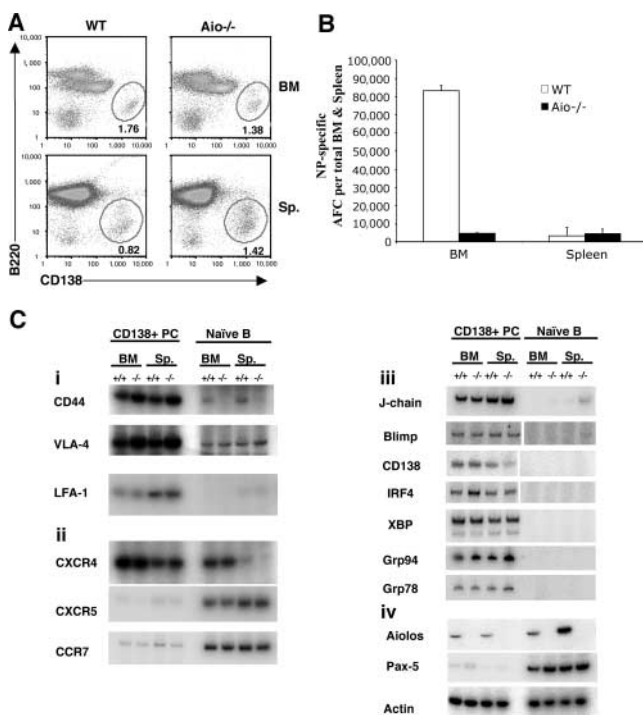

CXCR5 and CCR7 are normally down-regulated in GC B cells, whereas CXCR4, the receptor responsible for homing to the BM, remains high. A similar pattern of chemokine receptor expression was detected in WT and Aio$^{-/-}$ GC B cells (Fig. 5 E). It is still formally possible that AFC precursors, which comprise a very small subpopulation of the GC, are defective in BM homing due to deregulation in some other chemokine receptor.

Aio$^{-/-}$ Plasma Cells Express Normal Survival, Differentiation, and Homing Gene Profiles. Next, we examined the CD138$^+$ B220$^-$ population that is enriched in plasma cells. A slight decrease in the number of CD138$^+$ B220$^-$ cells was seen in the BM of Aio$^{-/-}$ mice 14 d after secondary immunization, whereas in the spleen there was an increase in this population (Fig. 6 A). ELISPOT analysis of the sorted cells, however, revealed a major deficiency in NP-specific AFC activity when obtained from the BM of Aio$^{-/-}$ mice (Fig. 6 B).

The CD138$^+$ B220$^-$ population was also examined for mRNA levels of genes involved in plasma cell survival, homing, and differentiation. Plasma cells have up-regulated cell surface expression of several adhesion molecules involved in their survival and homing (21). Expression of *CD44*, *VLA-4*, and *LFA-1* was increased in BM and splenic plasma cells compared with naive B cells. This increase was seen in CD138$^+$ B220$^-$ populations obtained from both WT and Aio$^{-/-}$ mice (Fig. 6 C, i). Consistent with our previous results (Fig. 5), the lymph node chemokine receptors CXCR5 and CCR7 were down-regulated in plasma cells, whereas they were expressed in naive B cells (Fig. 6 C, ii). CXCR4, in contrast, was up-regulated in splenic plasma cells compared with naive B cells, although there was some expression in BM naive B cells (Fig. 6 C, ii). No obvious difference in chemokine receptor expression was seen between WT and Aio$^{-/-}$ cells. Plasma cell function–associated genes *J-chain*, *Blimp*, *CD138*, *IRF4*, and *XBP-1* and ER stress genes *GRP78* and *GRP94* are increased in the CD138$^+$ cells with respect to naive B cells, and lack of Aiolos did not impair expression of any of these genes (Fig. 6 C, iii). In addition, down-regulation of *PAX5*, which is required for development of plasma cells (20), was seen in both WT and Aio$^{-/-}$ plasma cells (Fig. 6 C, iv). These results suggest that the lack of functional NP-specific AFCs in Aio$^{-/-}$ mice was not due to an inability to regulate previously described genes involved in general plasma cell differentiation, homing, or function. Rather, they support a model in which Aiolos is necessary for suitable plasma cell differentiation or function in the BM, possibly through unknown targets.

Discussion

Ag-specific Ab-secreting B cells generated during an immune response are thought to arise from distinct differentiation pathways and comprise a heterogeneous population with specific effector properties. It is the combination of these effector cells that is responsible for providing effective short-term and long-term immunity. Here we investigate the generation of plasma cells during the T cell–dependent
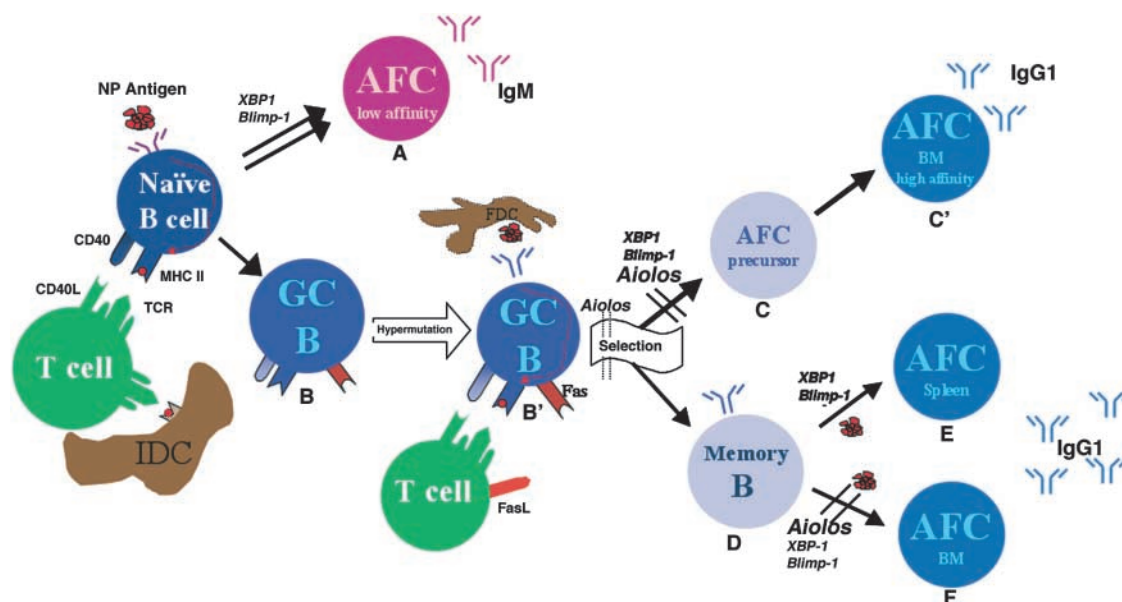
Figure 6. Examination of plasma cell–enriched populations for activity and expression of supporting factors. (A) FACS® analysis of BM (top) and spleen (bottom) cells from WT and Aio$^{-/-}$ mice 14 d after boost. Cells are gated within the non–B cell lineage compartment and stained with anti-B220 and anti-CD138 Abs. Percentages of plasma cell–like populations (B220$^-$ CD138$^+$) are circled and indicated. (B) Sorted B220$^-$ CD138$^+$ BM and spleen cells were analyzed by ELISPOT to determine their NP-specific AFC activity. Numbers reflect the amount of NP-specific AFCs per total organ, calculated as the number of AFCs/2,000 sorted and plated B220$^+$ CD138$^-$ cells, and adjusted for their percentage as given in A. Total cell counts for WT (open bars) and Aio$^{-/-}$ (solid bars) BM were similar. (C) RT-PCR analysis from sorted CD138$^+$ B220$^-$ cells from WT and Aio$^{-/-}$ mice. (i), expression of adhesion molecules *CD44*, *VLA-4*, and *LFA-1*; (ii), chemokine receptors *CXCR4*, *CXCR5*, and *CCR7*; (iii), plasma cell proteins *J-chain*, *Blimp*, *CD138*, *IRF-4*, *XBP*, stress response genes *Grp94* and *Grp78*; (iv), *Aiolos* message as well as B cell gene *PAX5* and the *actin* control.

Figure 7. Distinct pathways of plasma cell differentiation and their transcription factor requirements. The differentiation of a responding B cell to either a low affinity short-lived AFC (A) or a GC B cell (B) involves distinct pathways. The GC centroblast (B) undergoes somatic hypermutation of the Ig variable genes. Mutated centrocytes (B′) are selected for proper Ag binding and can further differentiate into a high affinity long-lived BM AFC (C–C′) or into a memory B cell (D) which recirculates throughout the body. Upon antigenic reexposure, the memory B cell rapidly differentiates into either a splenic short-lived AFC of high affinity (E) or a long-lived high affinity BM AFC (F). Aiolos is required for the differentiation of high affinity BM AFCs (C–C′ and F), whereas previously described nuclear factors like XBP-1 or Blimp-1 are required for differentiation of all AFC subsets.

immune response to NP in Aiolos-deficient mice and provide new insight into the regulatory requirements responsible for the generation of different plasma cell populations. The long-lived high affinity plasma cells that reside in the BM are absent in the Aiolos-deficient mice after both primary and secondary antigenic challenge. This indicates that a defect is manifested not only during the initial generation of this type of plasma cell from the GC, but also in their subsequent production from memory B cells. However, the short-lived low and high affinity plasma cell populations found in the spleen remain unaffected.

Early in the response, naïve B cells that have encountered Ag can directly differentiate into low affinity plasma cells (Fig. 7, population A). These plasma cells are found in the spleen and BM and constitute the first line of defense against pathogens. They have not undergone somatic hypermutation or isotype switching and disappear quickly after antigenic encounter. Aiolos deficiency does not interfere with this early and short-lived plasma cell response.

Later in the response, a high affinity plasma cell population accumulates in the BM (Fig. 7, population C′) that is long-lived and responsible for the long-term systemic production of high affinity Abs required for protective immunity. Lack of Aiolos selectively ablates this BM plasma cell population. Aio$^{-/-}$ mice show no significant number of plasma cells in the BM for several months after immunization, a period during which their number in the BM of WT mice has peaked. These findings indicate that there is no delay in the formation of AFCs. Thus, Aiolos is required for the generation of either a GC-derived high affinity AFC (Fig. 7, population C′) or a GC-derived AFC

precursor that homes to the BM (Fig. 7, population C). It is possible that Aiolos is necessary for the differentiation, homing, or survival of this population.

The presence of long-lived plasma cells in the BM is dependent on the GC reaction. Disruption of the GC by anti-CD40L Abs leads to a reduction of high affinity plasma cells in the BM while sparing the extrafollicular and low affinity subsets (22). Because formation of the high affinity BM plasma cells is impaired in Aio$^{-/-}$ mice, we examined whether there was a defect in the GC reaction. Previous experiments have shown the existence of GC in the spleens of aging unimmunized Aio$^{-/-}$ mice (12). Upon immunization, young Aio$^{-/-}$ mice show a similar increase in the number of GCs (not depicted). Thus, there is no intrinsic defect in the signals that drive B cell differentiation into a GC reaction in Aio$^{-/-}$ mice. Aio$^{-/-}$ GCs, however, appear to sustain B cell clones with decreased BCR affinity for Ag, as an increased number of noncanonical V(D)J rearrangements was recovered 13 d after primary immunization. Even within B cell clones with canonical sequences, changes reflective of antigenic selection such as high R/S ratios in CDR, W→L mutation at position 33, and usage of the YYGS/N motif in the CDR3, were decreased in Aio$^{-/-}$ GC B cells. Analysis of the 3′ flanking region of the V_H gene of GC B cells in Peyer's patches, which is not subject to selection, showed no defect in somatic hypermutation. Thus, there seems to be a relaxed negative selection in B cells from Aio$^{-/-}$ mice, allowing survival of low affinity GC B cells that would otherwise be lost during the primary response. This could be explained by the fact that Aio$^{-/-}$ B cells have decreased BCR signaling thresholds, allowing

survival of cells in Aio$^{-/-}$ mice that would have otherwise died by neglect in the GC.

Although there is a partial impairment in the selection of high affinity B cell clones in the GCs of Aio$^{-/-}$ mice, an altered level of signaling through the BCR is not likely to account for the severe reduction of plasma cells in the BM. There is recent evidence that very low affinity cells can undergo a GC reaction and mount AFC responses, and that low affinity plasma cell clones can survive long-term in the BM (23). In addition, FcγRIIB-deficient mice, whose B cells also display a hyperresponsive phenotype, have normal to increased humoral responses (24). As high affinity B cell clones are seen in the GCs of Aio$^{-/-}$ mice, one would expect some contribution from these cells to the BM plasma cell compartment, which is not the case. Furthermore, high affinity memory B cells (Fig. 2 A) are generated in normal numbers, indicating that B cells exiting the GC have undergone antigenic selection. Upon restimulation, these memory B cells (Fig. 7, population D) are responsible for the rapid but transient appearance of short-lived high affinity plasma cells in the spleen (Fig. 7, population E), resulting in a small temporal increase in high affinity anti–NP Ab titers. However, the BM plasma cell population remains severely impaired (Fig. 7, population F), suggesting that their deficit lies beyond the GC. Molecular analysis of sorted GC B cells supports this hypothesis because the expression of genes involved in clonal selection, survival, and plasma cell differentiation within the GC was normal in Aio$^{-/-}$ mice (Fig. 5). It is possible that the development of naive precursors of high affinity BM plasma cells are specifically affected by lack of Aiolos. Potential differences in the Aio$^{-/-}$ naive anti–NP repertoire relative to WT may also be responsible for the BM AFC deficit.

To determine whether the lack of BM plasma cells was due to a defect in homing or migration, AFC activity was assayed at other immunological sites. In mice deficient in the chemokine receptor CXCR4, homing of plasma cells or their precursors to the BM is impaired and plasma cells are found in elevated numbers in the blood and spleen of these mice for 2 wk after immunization (25). In Aio$^{-/-}$ mice, no increase in the number of NP-specific AFC activities was found in the blood or the lymph nodes. Examination of populations enriched for GC B and plasma cells as well as in vitro LPS-differentiated plasma cells revealed no defect in the expression of the chemokine receptors CXCR4, CXCR5, and CCR7 in Aio$^{-/-}$ cells. Expression of the adhesion molecules CD44, VLA-4, and LFA-1, which are up-regulated in plasma cells and involved in their stromal interaction (26), was also examined but no significant difference was found between Aio$^{-/-}$ and WT levels. Thus, it is unlikely that misexpression of these receptor and adhesion molecules causes altered homing or retention of plasma cells in the Aio$^{-/-}$ mice. It is possible that misexpression of other chemokine receptors with a potential role in plasma cell homing (27) is deregulated. Nonetheless, the low titer of high affinity NP-specific Abs in the serum of Aio$^{-/-}$ mice detected immediately to a few weeks after immunization correlates with the severe reduction of high affinity plasma cells and rules out an alternative site for their retention and short-term survival.

It is possible that BM plasma cells are generated in Aio$^{-/-}$ mice but are unable to survive due to a stromal defect. BM stroma was recently shown to be required for selection and survival of long-lived BM plasma cells (26, 28). In addition, stromal cells secrete IL-6, a growth factor required for plasma cell survival within the BM (26, 29). Reconstitution studies showed that Aio$^{-/-}$ B cells were not able to differentiate into plasma cells even in the presence of WT BM stroma (Fig. 4 C). These experiments rule out a stromal defect as the underlying cause of the AFC deficiency. Mixed chimera experiments have also confirmed that the plasma cell defect is intrinsic to the B cell compartment and not caused by insufficient help from Aio$^{-/-}$ T cells. These studies also rule out the possibility that plasma cell interactions with other BM B cells, which are altered in Aio$^{-/-}$ mice (i.e., pre-B/immature B; reference 12), were responsible for their BM AFC deficit.

Previous studies have shown that Ikaros and Aiolos are essential components of chromatin remodeling complexes within the nucleus that modulate the structure of chromatin to effect gene expression and control lymphocyte differentiation and proliferation (30–32). Gene expression studies on populations enriched for plasma cells and their precursors failed to reveal a major deficit in any of the previously described plasma cell differentiation factors. However, the low frequency of NP-specific plasma cells (∼1% of CD138$^+$ plasma cells in WT) could limit our ability to visualize changes in their gene expression profile within a heterogeneous plasma cell–like population. Therefore, we can only conclude that Aiolos does not affect expression of genes previously shown to be required for differentiation of all plasma cells. Another possibility is that Aiolos controls unidentified genes required for the differentiation or imminent survival of the long-lived high affinity plasma cell in the BM.

It has been recently shown that short- and long-lived plasma cells are derived from phenotypically distinct plasma cell precursor populations (33). This investigation provides further evidence that T cell–dependent generation of long-lived high affinity plasma cells occurs independently of other plasma cell subsets. It provides support for the hypothesis that these are a separate entity of Ab-secreting cells with a differentiation program that is distinct from that of short-lived high affinity as well as low affinity plasma cells. Future studies will aim to determine whether Aiolos is involved in generating and/or determining the fate of the plasma cell precursor populations. In contrast to the transcription factors *Blimp-1*, *XBP-1*, and *IRF4*, whose activities affect all plasma cells, *Aiolos* is the first transcription factor described to be specifically required for the differentiation and/or survival of the long-lived high affinity subset.

References

1. Takahashi, Y., P.R. Dutta, D.M. Cerasoli, and G. Kelsoe. 1998. In situ studies of the primary immune response to (4-hydroxy-3-nitrophenyl)acetyl. V. Affinity maturation develops in two stages of clonal selection. *J. Exp. Med.* 187:885–895.

2. Slifka, M.K., M. Matloubian, and R. Ahmed. 1995. Bone marrow is a major site of long-term antibody production after acute viral infection. *J. Virol.* 69:1895–1902.

3. Manz, R.A., A. Thiel, and A. Radbruch. 1997. Lifetime of plasma cells in the bone marrow. *Nature.* 388:133–134.

4. Jacob, J., R. Kassir, and G. Kelsoe. 1991. In situ studies of the primary immune response to (4-hydroxy-3-nitrophenyl)acetyl. I. The architecture and dynamics of responding cell populations. *J. Exp. Med.* 173:1165–1175.

5. Smith, K.G., T.D. Hewitson, G.J. Nossal, and D.M. Tarlinton. 1996. The phenotype and fate of the antibody-forming cells of the splenic foci. *Eur. J. Immunol.* 26:444–448.

6. Tarlinton, D.M., and K.G. Smith. 2000. Dissecting affinity maturation: a model explaining selection of antibody-forming cells and memory B cells in the germinal centre. *Immunol. Today.* 21:436–441.

7. McHeyzer-Williams, M.G., and R. Ahmed. 1999. B cell memory and the long-lived plasma cell. *Curr. Opin. Immunol.* 11:172–179.

8. Slifka, M.K., R. Antia, J.K. Whitmire, and R. Ahmed. 1998. Humoral immunity due to long-lived plasma cells. *Immunity.* 8:363–372.

9. Vieira, P., and K. Rajewsky. 1988. The half-lives of serum immunoglobulins in adult mice. *Eur. J. Immunol.* 18:313–316.

10. Ridderstad, A., and D.M. Tarlinton. 1998. Kinetics of establishing the memory B cell population as revealed by CD38 expression. *J. Immunol.* 160:4688–4695.

11. Morgan, B., L. Sun, N. Avitahl, K. Andrikopoulos, T. Ikeda, E. Gonzales, P. Wu, S. Neben, and K. Georgopoulos. 1997. Aiolos, a lymphoid restricted transcription factor that interacts with Ikaros to regulate lymphocyte differentiation. *EMBO J.* 16:2004–2013.

12. Wang, J.H., N. Avitahl, A. Cariappa, C. Friedrich, T. Ikeda, A. Renold, K. Andrikopoulos, L. Liang, S. Pillai, B.A. Morgan, et al. 1998. Aiolos regulates B cell activation and maturation to effector state. *Immunity.* 9:543–553.

13. Cariappa, A., M. Tang, C. Parng, E. Nebelitskiy, M. Carroll, K. Georgopoulos, and S. Pillai. 2001. The follicular versus marginal zone B lymphocyte cell fate decision is regulated by Aiolos, Btk, and CD21. *Immunity.* 14:603–615.

14. Sun, J., G. Matthias, M.J. Mihatsch, K. Georgopoulos, and P. Matthias. 2003. Lack of the transcriptional coactivator OBF-1 prevents the development of systemic lupus erythematosus-like phenotypes in Aiolos mutant mice. *J. Immunol.* 170:1699–1706.

15. Jolly, C.J., N. Klix, and M.S. Neuberger. 1997. Rapid methods for the analysis of immunoglobulin gene hypermutation: application to transgenic and gene targeted mice. *Nucleic Acids Res.* 25:1913–1919.

16. Takahashi, Y., H. Ohta, and T. Takemori. 2001. Fas is required for clonal selection in germinal centers and the subsequent establishment of the memory B cell repertoire. *Immunity.* 14:181–192.

17. Jacob, J., J. Przylepa, C. Miller, and G. Kelsoe. 1993. In situ studies of the primary immune response to (4-hydroxy-3-nitrophenyl)acetyl. III. The kinetics of V region mutation and selection in germinal center B cells. *J. Exp. Med.* 178:1293–1307.

18. Cumano, A., and K. Rajewsky. 1986. Clonal recruitment and somatic mutation in the generation of immunological memory to the hapten NP. *EMBO J.* 5:2459–2468.

19. Calame, K.L. 2001. Plasma cells: finding new light at the end of B cell development. *Nat. Immunol.* 2:1103–1108.

20. Angelin-Duclos, C., G. Cattoretti, K.I. Lin, and K. Calame. 2000. Commitment of B lymphocytes to a plasma cell fate is associated with Blimp-1 expression in vivo. *J. Immunol.* 165:5462–5471.

21. Underhill, G.H., H.A. Minges Wols, J.L. Fornek, P.L. Witte, G.S. Kansas, and H.A. Minges-Wols. 2002. IgG plasma cells display a unique spectrum of leukocyte adhesion and homing molecules. *Blood.* 99:2905–2912.

22. Han, S., K. Hathcock, B. Zheng, T.B. Kepler, R. Hodes, and G. Kelsoe. 1995. Cellular interaction in germinal centers: roles of CD40 ligand and B7-2 in established germinal centers. *J. Immunol.* 155:556.

23. Takahashi, Y., D.M. Cerasoli, J.M. Dal Porto, M. Shimoda, R. Freund, W. Fang, D.G. Telander, E.N. Malvey, D.L. Mueller, T.W. Behrens, et al. 1999. Relaxed negative selection in germinal centers and impaired affinity maturation in bcl-xL transgenic mice. *J. Exp. Med.* 190:399–410.

24. Takai, T., M. Ono, M. Hikida, H. Ohmori, and J.V. Ravetch. 1996. Augmented humoral and anaphylactic responses in Fc gamma RII-deficient mice. *Nature.* 379:346–349.

25. Hargreaves, D.C., P.L. Hyman, T.T. Lu, V.N. Ngo, A. Bidgol, G. Suzuki, Y.R. Zou, D.R. Littman, and J.G. Cyster. 2001. A coordinated change in chemokine responsiveness guides plasma cell movements. *J. Exp. Med.* 194:45–56.

26. Minges Wols, H.A., G.H. Underhill, G.S. Kansas, and P.L. Witte. 2002. The role of bone marrow-derived stromal cells in the maintenance of plasma cell longevity. *J. Immunol.* 169:4213–4221.

27. Hauser, A.E., G.F. Debes, S. Arce, G. Cassese, A. Hamann, A. Radbruch, and R.A. Manz. 2002. Chemotactic responsiveness toward ligands for CXCR3 and CXCR4 is regulated on plasma blasts during the time course of a memory immune response. *J. Immunol.* 169:1277–1282.

28. Manz, R.A., and A. Radbruch. 2002. Plasma cells for a lifetime? *Eur. J. Immunol.* 32:923–927.

29. Han, S., K. Yang, Z. Ozen, W. Peng, E. Marinova, G. Kelsoe, and B. Zheng. 2003. Enhanced differentiation of splenic plasma cells but diminished long-lived high-affinity bone marrow plasma cells in aged mice. *J. Immunol.* 170:1267–1273.

30. Kim, J., S. Sif, B. Jones, A. Jackson, J. Koipally, E. Heller, S. Winandy, A. Viel, A. Sawyer, T. Ikeda, et al. 1999. Ikaros DNA-binding proteins direct formation of chromatin remodeling complexes in lymphocytes. *Immunity.* 10:345–355.

31. Avitahl, N., S. Winandy, C. Friedrich, B. Jones, Y. Ge, and K. Georgopoulos. 1999. Ikaros sets thresholds for T cell activation and regulates chromosome propagation. *Immunity.* 10:333–343.

32. Harker, N., T. Naito, M. Cortes, A. Hostert, S. Hirschberg, M. Tolaini, K. Roderick, K. Georgopoulos, and D. Kioussis. 2002. The CD8alpha gene locus is regulated by the Ikaros family of proteins. *Mol. Cell.* 10:1403–1415.

33. O'Connor, B.P., M. Cascalho, and R.J. Noelle. 2002. Short-lived and long-lived bone marrow plasma cells are derived from a novel precursor population. *J. Exp. Med.* 195:737–745.